Available online at www.sciencedirect.com
ScienceDirect
Applied Surface Science 253 (2007) 7398–7403
applied surface science
www.elsevier.com/locate/apsusc

Transparent and conducting Zn-Sn-O thin films prepared by combinatorial approach

J.H. Ko [a], I.H. Kim [a], D. Kim [b], K.S. Lee [a], T.S. Lee [a], B. Cheong [a], W.M. Kim [a,*]

[a] Thin Film Materials Research Center, Korea Institute of Science and Technology, 39-1, Hawolgok-dong, Sungbuk-gu, Seoul 136-791, Republic of Korea
[b] Division of Materials Science and Engineering, Korea University, Anam-Dong 5-1, Sungbuk-gu, Seoul 136-701, Republic of Korea

Received 6 December 2006; received in revised form 9 March 2007; accepted 15 March 2007
Available online 24 March 2007

Abstract

Zn-Sn-O (ZTO) films with continuous compositional gradient of Sn 16–89 at.% were prepared by co-sputtering of two targets of ZnO and SnO_2 in a combinatorial method. The resistivities of the ZTO films were severely dependent on oxygen content in sputtering gas and Zn/Sn ratio. Except for the films with Sn 16 at.%, all the as-prepared films were amorphous and maintaining the stable amorphous states up to the annealing temperature of 450 °C. Annealing at 650 °C resulted in crystallization for all the composition, in which ZnO, Zn_2SnO_4, $ZnSnO_3$, and SnO_2 peaks were appeared successively with increasing Sn content. Above Sn 54 at.%, the ZTO films were deduced to have a local structure mixed with $ZnSnO_3$ and SnO_2 phases which were more conductive and stable in thermal oxidation than ZnO and Zn_2SnO_4 phases. The lowest resistivity of 1.9×10^{-3} Ω cm was obtained for the films with Sn 89 at.% when annealed at 450 °C in a vacuum. The carrier concentrations of the amorphous ZTO films that contained Sn contents higher than 36 at.% and annealed at 450 °C in a vacuum were proportional to the Sn contents, while the Hall mobilities were insensitive to Sn contents and leveling in the range of 23–26 cm^2/V s.

PACS : 73.61.−r: 78.20−e

Keywords: Zinc tin oxide; Amorphous; Transparent conducting oxide; Thin film

1. Introduction

Transparent conducting oxide (TCO) films are materials which are highly transparent to visible light and electrically conductive. TCOs have been used in many applications as transparent electrodes of flat-panel devices, solar cells, and infra-red (IR) reflectors. During the last 30–40 years, most research has been focused on binary compounds such as In_2O_3, ZnO, and SnO_2. Recently, amorphous multicomponent oxides such as In-Zn-O (IZO) and Zn-Sn-O (ZTO) systems have attracted much attention as mew TCO materials [1–4]. Since amorphous TCO thin films have smoother surface morphology [5] and cleaner etched profiles compared with crystalline TCO films [6], amorphous TCO films have inherent advantages for applications such as organic light emitting diode (OLED) and thin film transistor–liquid crystal display (TFT–LCD) if appropriate electrical and optical properties can be obtained. Although IZO thin films have been proved to have relatively good electrical properties, they have drawbacks due to the fact that the major constituent is indium, which is scarce and expensive, and that the surface properties are not good enough to be used for device application [6]. Unlike the IZO thin films, amorphous ZTO films have not been studied extensively. Although ZTO films are known to have a demerit of difficulty in chemical etching, especially at high Sn concentration, they may still be able to find their usefulness for certain applications as an alternative TCO material due to their virtues. These virtues are that the constituents of zinc and tin are much cheaper than indium, and that the film properties can be tailored to have both the advantage of good thermal stability and mechanical strength for SnO_2 and the advantage of good stability under the reducing atmosphere for ZnO.

In this study, ZTO films with continuous compositional variation over the position of substrates were prepared by co-sputtering two targets of ZnO and SnO_2 following a combinatorial approach [2]. The predominant local structure

* Corresponding author. Tel.: +82 2 958 5384; fax: +82 2 958 5409.
E-mail address: wmkim@kist.re.kr (W.M. Kim).

0169-4332/$ – see front matter © 2007 Elsevier B.V. All rights reserved.
doi:10.1016/j.apsusc.2007.03.036

as the function of Sn/(Zn + Sn) and the corresponding changes of electrical and optical properties were investigated.

2. Experimental details

ZTO films were deposited on glass substrates (Corning Eagle 2000 and soda lime glass) by radio frequency (rf) magnetron sputtering of two 2-in. diameter targets of pure ZnO (99.99% purity) and SnO_2 (99.99% purity) in a combinatorial method [2]. Fig. 1 is the schematic diagram of the combinatorial sputtering adopted in this study showing the arrangement of two magnetron cathodes angled toward the center of the substrate. Due to the relative difference in fluxes of sputtered particles from two targets, the deposited films have continuously varying compositions of Zn and Sn metal components. The rf power of ZnO and SnO_2 were kept at 40 and 38 W, respectively, at which the deposited films had the analogous deposition rate. Seven glass substrates were mounted on the sample holder in a single row and in parallel with the two targets. The glass substrates, which have the narrow width size of 10 mm × 20 mm, were designed to minimize the thickness difference of positioned samples. The base pressure in the chamber was below 5×10^{-5} Pa and the sputtering deposition was carried out at a pressure of 0.13 Pa with pure Ar gas and a gas mixture of Ar and oxygen. The substrate was not intentionally heated.

Film thicknesses were measured from the films deposited on strip-masked substrates using a profilometer (model Alpha-step 200, Tencor). For compositional analysis, electron-probe microanalysis (EPMA) characterization was made for the as-prepared films. The electrical resistivities, Hall mobilities, and carrier concentrations were determined from Hall-effect measurement equipment using a Van der Pauw method. Crystalline structures of the films were analyzed using an X-ray diffractometer (Mac Science). The chemical shifts of the Zn 2p and Sn 3d peaks were measured by X-ray photoelectron spectroscopy (XPS, PHI 5800) with Al Kα X-rays. The optical transmission and reflection spectra were obtained on a Shimadzu UV-3101 PC spectrophotometer in wavelength ranges of 250–1100 nm. Annealing treatments of as-prepared films were carried out in a vacuum of about 1 Pa and air at 450 and 650 °C for 1 h, respectively.

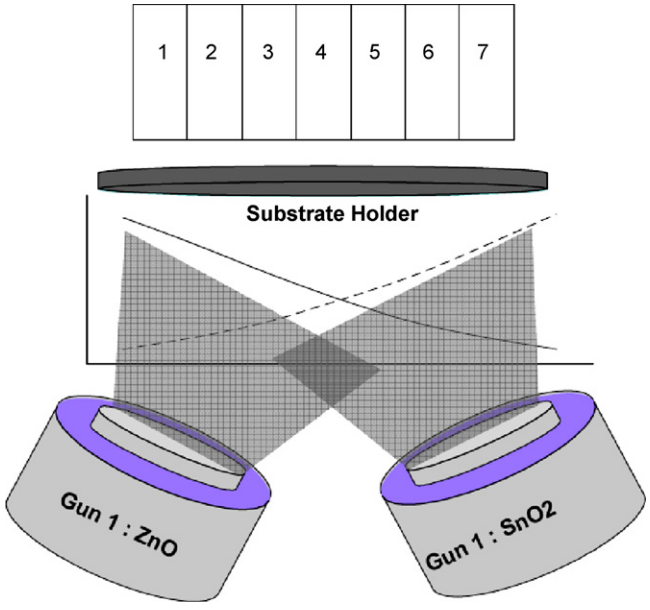

Fig. 1. Schematic diagram of combinatorial sputtering and configuration of substrates.

3. Results and discussion

Fig. 2(a) shows film thickness profiles of the ZTO films deposited in sputtering gas containing four different oxygen contents. The leftmost film position 1 is near the ZnO target and the rightmost film position 7 is near the SnO_2 target. The thickness of as-prepared ZTO films obtained in combinatorial configuration was slightly different from the sum of each ZnO and SnO_2 films thickness measured in single-target sputtering. This may be due to the interference of the plasma during co-sputtering. For the measurement of electrical properties, the film position 4 with minimum film thickness was set to 200 nm, giving the corresponding thickness of film position 1 and 7 to be about 250 and 300 nm, respectively. Fig. 2(b) summarizes the electrical resistivities of ZTO films deposited in sputter gas containing different oxygen content plotted against film

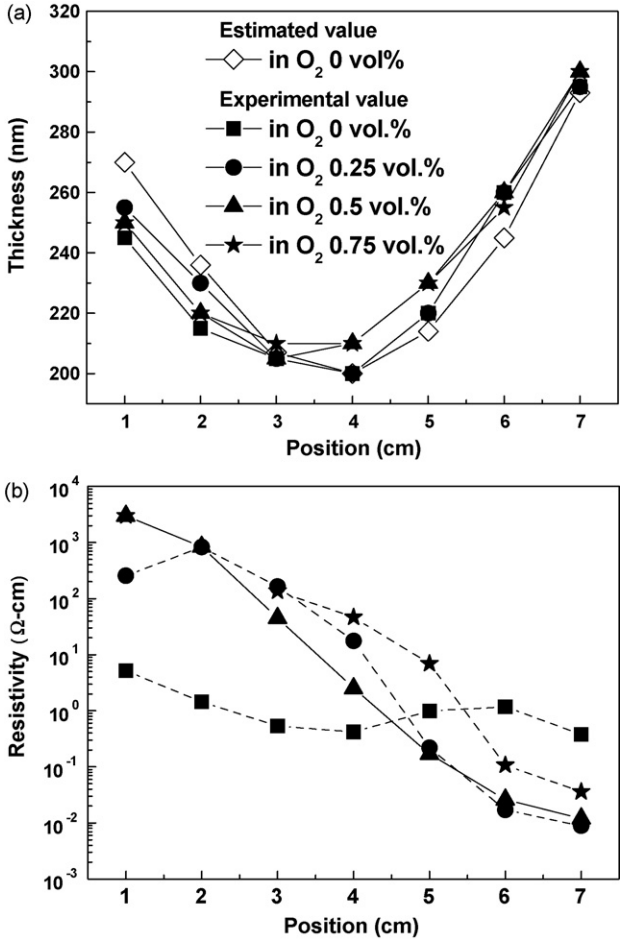

Fig. 2. (a) Film thickness profiles and (b) electrical resistivities of the ZTO films deposited in sputtering gas containing four different oxygen contents.

position, i.e. Zn/Sn ratio. The Sn-rich films deposited in the pure Ar were brown colored and had relatively high resistivities. With increasing oxygen content, all the films became transparent and the resistivities of Zn-rich films increased, while the resistivities of Sn-rich films decreased. It is noticeable that the oxygen content in sputter gas is one of the crucial parameters determining the electrical properties of the films for a given composition. It has been reported that the highly resistive and brownish SnO_x films mixed with multi-phases such as SnO and Sn_3O_4 were obtained when the films were deposited at a low oxygen partial pressure [7]. However, ZnO thin films deposited at a high-oxygen partial pressure were highly resistive, suppressing carrier generation via oxygen-vacancy formation because the Zn ion forms stronger chemical bonds with oxygen than with the Sn ion [8]. The oxygen content of 0.5% by volume in sputtering gas used in our experiment is an adequate amount for obtaining highly conductive Sn-rich films. Thus further analyses were made using the films deposited with sputter gas containing 0.5 vol.% of oxygen on the Corning glass substrates.

In Fig. 3, the compositional results obtained from EPMA analysis on the as-prepared films deposited with sputter gas containing 0.5 vol.% of oxygen are plotted. The behavior of measured Sn at.% followed Sn content estimated from the deposition rate of single-target sputtering. However, for all the film compositions, the contents of Sn measured by EPMA were slightly higher than estimated values. A similar observation has been reported by Minami et al. [1]. It must be mentioned at this point that the composition designated at each sample position is not the one averaged over the sample area, but instead the one obtained from the central portion of each sample. In the following analysis, the structural and the optical analyses of each film were also made on the central portion of the sample so that the compositional values could represent the corresponding structural and optical properties of the films as much as possible. The electrical properties obtained using Van der Pauw method, however, could not avoid finding averaged properties over the sample area due to the inevitable characteristics of this measurement method. Therefore, there might be a slight discrepancy in correlating the electrical properties of each film with the corresponding composition because the composition was not exactly in linear relation with respect to the sample position, although the difference would not be large enough to mislead the overall behavior of electrical properties with composition.

Although three sets of combinatorial samples, which were fabricated at an identical sputter condition, were used for the following analysis, the compositional analysis was made for just one set of samples. For all three sets, however, the compositional variation is thought to be almost same, because the behaviors of the electrical resistivity and the thickness in these three sets were similar to each other. Considering the positional, i.e. the compositional dependence of resistivities of ZTO samples deposited with sputter gas containing 0.5 vol.% of oxygen, even small deviations in composition would have lead to large differences in resistivity.

Fig. 4(a and b) contains X-ray diffraction (XRD) profiles of ZTO films annealed in vacuum at 450 and 650 °C for 1 h,

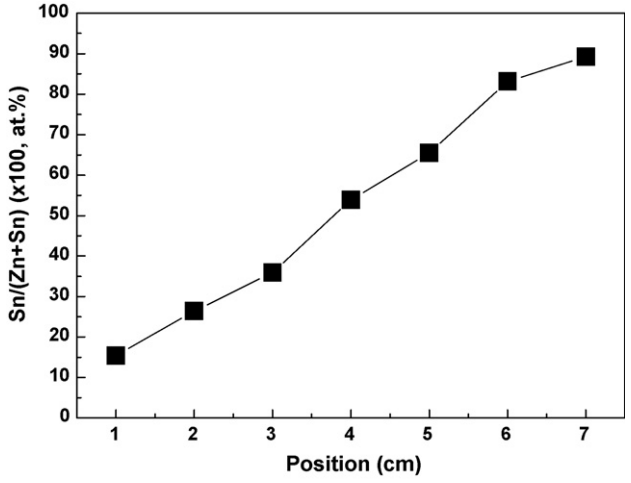

Fig. 3. Sn at.% of as-prepared ZTO films over the substrates measured by EPMA.

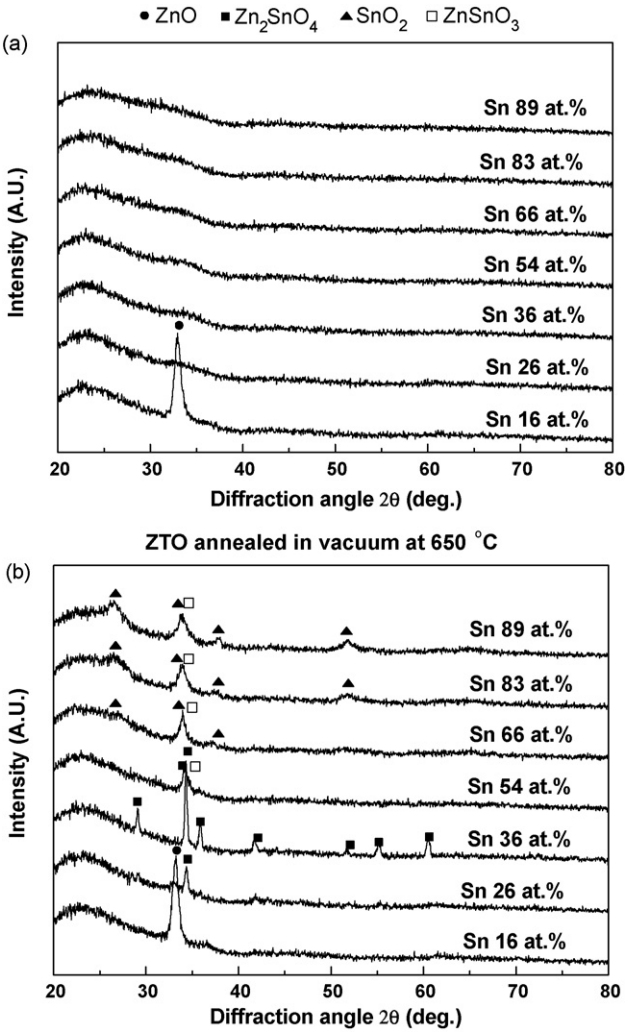

Fig. 4. XRD profiles of ZTO films annealed at (a) 450 °C and (b) 650 °C in vacuum.

respectively. The XRD profiles of the as-prepared ZTO films are not provided because they were almost the same as those of ZTO films annealed at 450 °C. Except for the ZTO film with Sn 16 at.%, all the as-prepared ZTO films exhibited the characteristic profile of an amorphous structure stable up to 450 °C and crystallized at 650 °C. The ZTO film with Sn 16 at.% showed only the (0 0 2) peak of ZnO. As Sn content reached 26 at.%, a weak Zn_2SnO_4(3 1 1) peak of an inverse-spinel structure appeared while the (0 0 2) peak of ZnO was disappeared. Weak and broad Zn_2SnO_4 peaks of the inverse-spinel structure were found for films in the range of Sn 26–54 at.%. The single phase of Zn_2SnO_4 was especially observed for the film with Sn 36 at.%. For films with higher Sn content than 54 at.%, peaks from SnO_2 or $ZnSnO_3$ started appearing while peaks of Zn_2SnO_4 disappearing. It was noticeable that the (3 1 1) peak of Zn_2SnO_4 appeared at 2θ value near 34.3°, while the most intensive peaks from the films with higher Sn contents than 66 at.% appeared at 2θ value near 33.9°. Broad and weak peaks were observed in all the crystallized films, resulting in poor crystallinity, which indicated that the size of crystallites within the film did not exceed a diameter of about 8 nm. It is rather difficult to discern the presence of the $ZnSnO_3$ phase in the films with high Sn content from XRD profiles only because the major peak positions from SnO_2 and $ZnSnO_3$ superimpose over each other [9,10].

Fig. 5 shows the XPS spectra of (a) Zn $2p_{3/2}$ and (b) Sn $3d_{5/2}$ core shells obtained from the amorphous (as-prepared) and the crystallized (annealed at 650 °C) films containing 36 and 66 Sn at.%. The XPS spectra were obtained after pre-cleaning the sample surface in argon plasma to exclude surface contamination. The binding energies were calibrated by taking the C 1s peak (254.8 eV) as a reference [11]. As for both the Zn $2p_{3/2}$ and Sn $3d_{5/2}$ peak positions, there were noticeable peak shifts toward the higher binding energy of the ZTO film with 66 Sn at.% when compared to the shifts obtained from the films containing 36 at.% Sn whose local structure was Zn_2SnO_4, implying that a different local structure from Zn_2SnO_4 was present in the film with Sn 66 at.%. Furthermore, the peak positions of Zn $2p_{3/2}$ of the ZTO film with Sn 66 at.% are different from those obtained from pure ZnO film. The relative shifts of peak positions observed from the XPS spectra of Zn $2p_{1/2}$ and Sn $3d_{3/2}$ were almost the same as those of Zn $2p_{3/2}$ and Sn $3d_{5/2}$. Combining the observations from the XRD profiles and the XPS spectra leads to a deduction that the chemical states of Zn in the ZTO films with Sn contents larger than 56 at.% are related with not Zn_2SnO_4 or ZnO phases but instead to the $ZnSnO_3$ phase. Also, it is notable from the XPS spectra that the relative peak positions and intensities from the amorphous films coincided with those from the crystallized films for a given composition, indicating that the chemical surroundings in the amorphous films are similar to those in the crystallized films of the corresponding composition. Thus, the perceived local structures in the amorphous ZTO films might be $(ZnO)_{1-X}(SnO_2)_X$, $(Zn_2SnO_4)_{1-X}(ZnO)_X$, Zn_2SnO_4, $(ZnSnO_3)_{1-X}(Zn_2SnO_4)_X$, and $(ZnSnO_3)_{1-X}(SnO_2)_X$ in Sn 16, 26, 36, 54 at.%, and in the range of Sn 66–89 at.%, respectively.

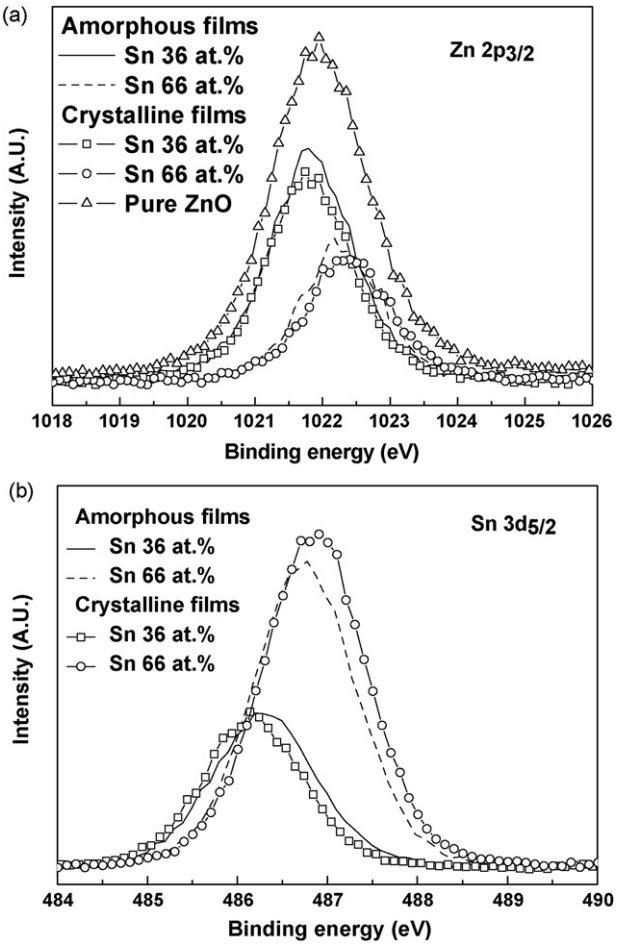

Fig. 5. XPS spectra of (a) Zn $2p_{3/2}$ and (b) Sn $3d_{5/2}$ core shells obtained from the amorphous (as-prepared) and the crystallized (annealed at 650 °C) films containing 36 and 66 Sn at.%. For comparison, the spectrum from pure ZnO is also included in the Zn $2p_{3/2}$ spectra.

Fig. 6 summarizes (a) the electrical resistivities, (b) carrier concentrations, and (c) Hall mobilities of the ZTO films as-deposited and post-annealed at 450 and 650 °C. The resistivities of the as-prepared amorphous ZTO films decreased when increasing the Sn contents. For the ZTO films with Sn 16 and 26 at.%, the definite Hall voltages were not obtained because of high resistivities. Upon annealing in a vacuum at 450 °C, the resistivities of ZTO films decreased remarkably compared with the as-prepared films. This occurred mainly due to the increase of the carrier concentrations. The relative extent of the increase in the carrier concentrations decreased with increasing Sn content, indicating that the free carriers might be generated by the oxygen vacancies and that the oxygens affect the Zn-rich films more than the Sn rich-films. For the ZTO films with Sn 16, 26, and 36 at.% the carrier concentrations were almost the same values. However, the carrier concentration increased when the Sn content was increased above 36 at.% and reached 1.4×10^{20} cm^{-3}, resulting in the minimum resistivity of 1.9×10^{-3} Ω cm in the film with Sn 89 at.%. It was perceived that the predominant local structures of the amorphous ZTO films with Sn 16, 26, and 36 at.% were the mixtures of ZnO and

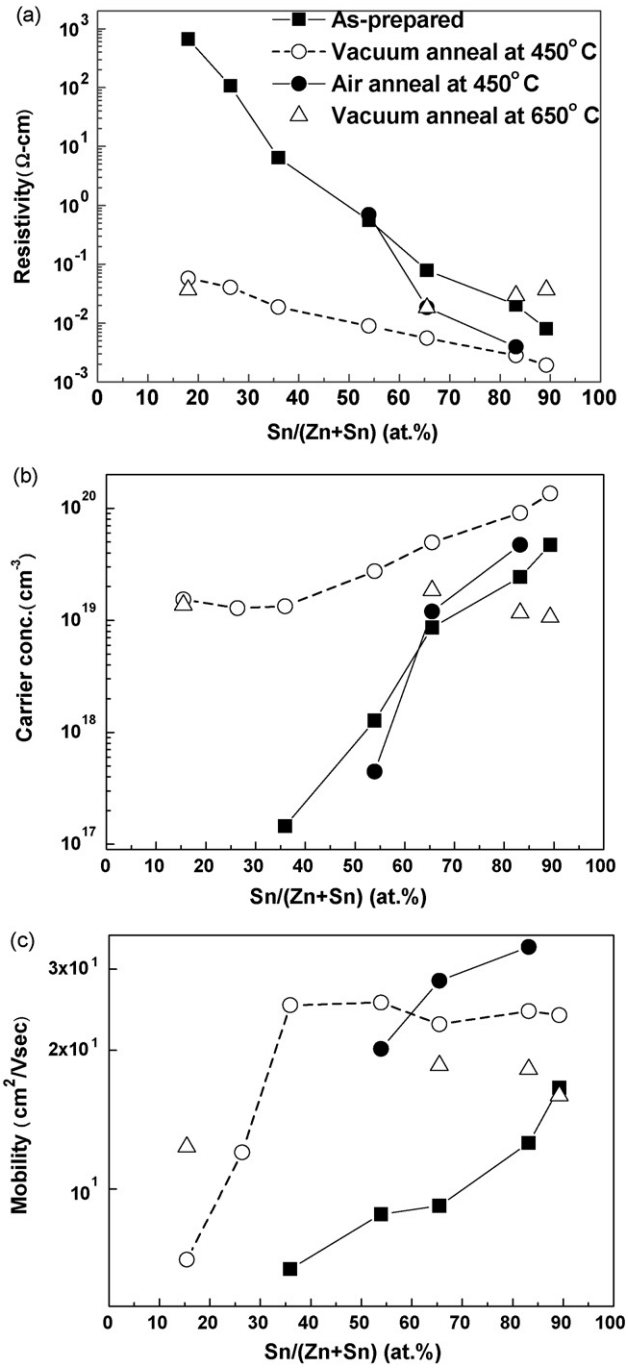

Fig. 6. Electrical properties of the as-deposited and the annealed ZTO films: (a) resistivities, (b) carrier concentrations, and (c) Hall mobilities.

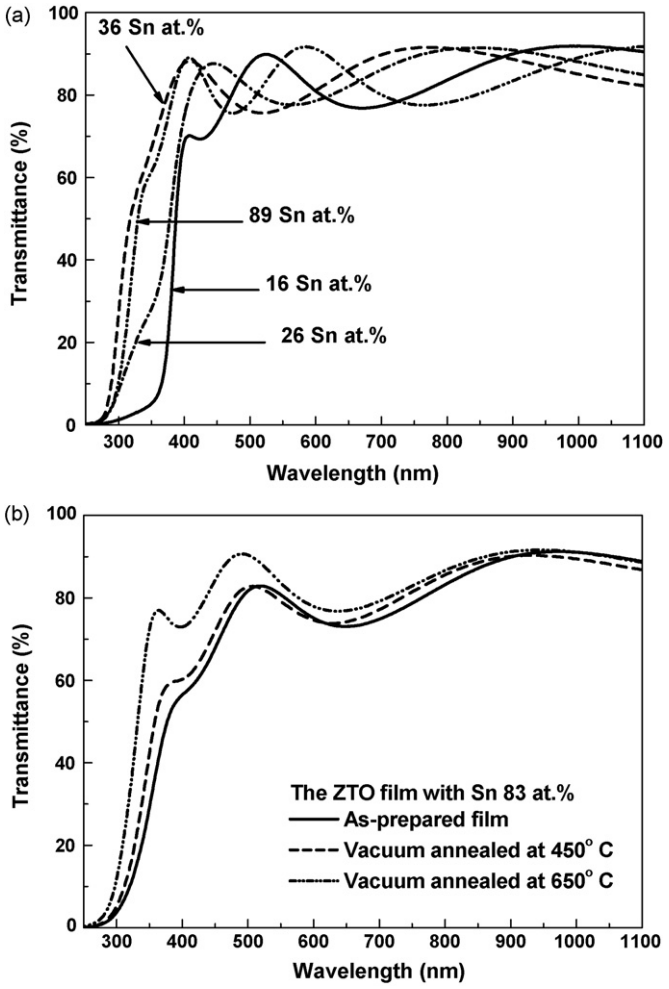

Fig. 7. Optical-transmission spectra of (a) the crystallized ZTO films annealed in vacuum at 650 °C for Sn 16, 26, 36, and 89 at.%, and (b) the ZTO film with Sn 83 at.% as-prepared and annealed in vacuum at 450 and 650 °C.

Zn_2SnO_4. For ZTO films with higher Sn content than 54 at.%, the SnO_2 and $ZnSnO_3$ phase might be formed. Combining these behaviors of the carrier concentration and the perceived local structure leads us to believe that the free carriers were easily generated from oxygen vacancies around SnO_2 and $ZnSnO_3$ phases, which were more conductive than ZnO and Zn_2SnO_4 phases. This result is well matched with the results observed by Moriga and Minami [1,3]. Moreover, upon annealing in the air at 450 °C, the definite Hall voltages were only observed in the ZTO films with the range of Sn 54–83 at.%. The maximum Hall mobility of 34 $cm^2/V\,s$ was obtained for the film with Sn 83 at.%. This finding implies that $ZnSnO_3$ and SnO_2 phases are much more stable against thermal oxidation than ZnO and Zn_2SnO_4 phase [1,12].

In contrast with the behaviors of the carrier concentrations, the Hall mobilities of ZTO films annealed in the vacuum at 450 °C increased very sharply with increasing Sn contents until the Sn content reached 36 at.%., and kept at almost the constant level in the range of 23–26 $cm^2/V\,s$ for films with Sn content above 36 at.%. It is interesting to note that the Hall mobility of the amorphous ZTO annealed at 450 °C in vacuum is insensitive to the Zn/Sn ratio and the value of Hall mobility is rather high compared with those observed from the amorphous semiconductors such as a-Si, amorphous chalcogenide, and V_2O_3 [13,14]. It has been reported that the mobilities of the amorphous metal oxides composed of heavy metal cations with an electronic configuration $(n-1)d^{10}ns^0$ $(n \geq 4)$ are insensitive to the structural disorder because of the large overlap between ns orbitals with spherical symmetry [14]. Thus, for the amorphous films with Sn content above 36 at.%, the high and constant values of Hall mobilities were attributed

to the well-formed conduction paths due to the overlapping of Sn 5s and Zn 4s orbitals.

After annealing in vacuum at 650 °C, except for the ZTO film with Sn 16 at.%, the resistivities of all the crystallized ZTO films increased. This resulted from the decrease of carrier concentrations and Hall mobilities compared to the amorphous ZTO films annealed at 450 °C. The resistivities of the ZTO films with Sn 26, 36, and 54 at.% were too high to be measured by a Van der Pauw technique. Accompanying the transition from the amorphous to the crystalline phase, it is expected that the broad grain boundaries were formed because of the low crystallinity. Thus the free carriers were trapped in these grain boundaries and the double-Schottky potential barriers were formed, resulting in the decrease of carrier concentrations and mobilities [15].

Fig. 7(a) shows the optical-transmission spectra of the crystallized ZTO films annealed in a vacuum at 650 °C. The absorption edges of the ZTO films moved toward the shorter wavelengths with increasing Sn contents. The ZTO films with Sn 36 at.%, whose predominant structure was Zn_2SnO_4, had the shortest absorption edge. The ZTO films composed of the mixtures of $ZnSnO_3$ and SnO_2 and with Sn composition equal to and larger than 54 at.% had absorption edges similar to each other. This behavior of the absorption edges likely arises from the compositional or structural variations of the ZTO films; the optical band gap of SnO_2 has been reported to be higher than that of ZnO [16]. Fig. 7(b) shows the changes in the optical-transmission spectra of the ZTO film with Sn 83 at.% with increasing annealing temperature in a vacuum. The shift of the absorption edges toward the shorter wavelengths upon annealing at 450 °C was attributed to the Burstein–Moss effects resulting from the increase of the carrier concentrations. The crystallization of amorphous ZTO films was accompanied with a remarkable shift of the absorption edges toward the shorter wavelength due to the reduction of extended- to localized-state transitions which resulted from the band tail formed due to the defect or disorderliness [12]. The optical-transmittances of ZTO films were between 75 and 90% in the visible wavelength.

4. Conclusions

In this work, ZTO films with the wide composition ranges of Sn 16–89 at.% were prepared utilizing a combinatorial sputtering mode. Except for the film with Sn 16 at.%, all the as-prepared films were amorphous and maintained the stable amorphous states up to the annealing temperature of 450 °C. With increasing Sn content, the perceived predominant local structure changed from ZnO and Zn_2SnO_4 to $ZnSnO_3$ and SnO_2 phases successively. $ZnSnO_3$ and SnO_2 phases were more conductive than ZnO and Zn_2SnO_4 phases and showed good stability against high-temperature oxidation. As a result, the amorphous ZTO films composed of SnO_2 and $ZnSnO_3$ phases may be good candidates for new TCO materials.

References

[1] T. Minami, S. Takata, H. Sato, H. Sonohara, J. Vac. Sci. Technol. A 13 (3) (1995) 1095.
[2] J.D. Perkins, J.A. del Cueto, J.L. Alleman, C. Warmsingh, B.M. Keyes, L.M. Gedvilas, P.A. Parilla, B. To, D.W. Readey, D.S. Ginley, Thin Solid Films 411 (2002) 152.
[3] T. Moriga, Y. Hayashi, K. Kondo, Y. Nishimura, K. Murai, I. Nakabayashi, J. Vac. Sci. Technol. A 22 (4) (2004) 1705.
[4] T. Moriga, T. Okamoto, K. Hiruta, A. Fujiwara, I. Nakayabashi, K. Tominaga, J. Solid State Chem. 155 (2000) 312.
[5] W.M. Kim, D.Y. Ku, I. Lee, Y.W. Seo, B. Cheong, T.S. Lee, I. Kim, K.S. Lee, Thin Solid Films 473 (2005) 315.
[6] G.S. Chae, Jpn. J. Appl. Phys. 40 (2001) 1282.
[7] A. Martel, F. Caballero-Briones, P. Bartolo-Perez, A. Iribarren, R. Castro-Rodriguez, A. Zapata-Navarro, J.L. Pena, Surf. Coat. Technol. 148 (2001) 103.
[8] T. Tsuji, M. Hirohashi, Appl. Surf. Sci. 157 (2000) 47.
[9] H.Q. Chiang, J.F. Wager, R.L. Hoffman, J. Jeong, D.A. Keszler, Appl. Phys. Lett. 86 (2005) 13503.
[10] S. Yu-Sheng, Z. Tian-Shu, Sens. Actuators B 52 (1998) 251.
[11] J.F. Moulder, W.F. Stickle, P.E. Sobol, K.D. Bomben, Handbook of X-ray Photoelectron Spectroscopy Physical Electronics, Eden Prarie, Minnesota, 1995.
[12] D.L. Young, Ph.D. Thesis, Colorado School of Mines, 2000.
[13] H. Hosnono, M. Yasukawa, H. Kawazoe, J. Non-Cryst. Solids 203 (1996) 334.
[14] M. Orita, H. Ohta, M. Hirano, S. Narushima, H. Hosono, Philos. Magn. B 81 (5) (2001) 501.
[15] K.L. Chopra, S. Major, D.K. Pandya, Thin Solid Films 102 (1983) 1.
[16] K. Ellmer, J. Phys. D: Appl. Phys. 34 (2001) 3097.